ACS OMEGA

Open Access

http://pubs.acs.org/journal/acsodf

Article

Exact Non-Markovian Quantum Dynamics on the NISQ Device Using Kraus Operators

Avin Seneviratne, Peter L. Walters, and Fei Wang*

Cite This: *ACS Omega* 2024, 9, 9666−9675

Read Online

ACCESS | Metrics & More | Article Recommendations | Supporting Information

ABSTRACT: The theory of open quantum systems has many applications ranging from simulating quantum dynamics in condensed phases to better understanding quantum-enabled technologies. At the center of theoretical chemistry are the developments of methodologies and computational tools for simulating charge and excitation energy transfer in solutions, biomolecules, and molecular aggregates. As a variety of these processes display non-Markovian behavior, classical computer simulation can be challenging due to exponential scaling with existing methods. With quantum computers holding the promise of efficient quantum simulations, in this paper, we present a new quantum algorithm based on Kraus operators that capture the exact non-Markovian effect at a finite temperature. The implementation of the Kraus operators on the quantum machine uses a combination of singular value decomposition (SVD) and optimal Walsh operators that result in shallow circuits. We demonstrate the feasibility of the algorithm by simulating the spin-boson dynamics and the exciton transfer in the Fenna−Matthews−Olson (FMO) complex. The NISQ results show very good agreement with the exact ones.

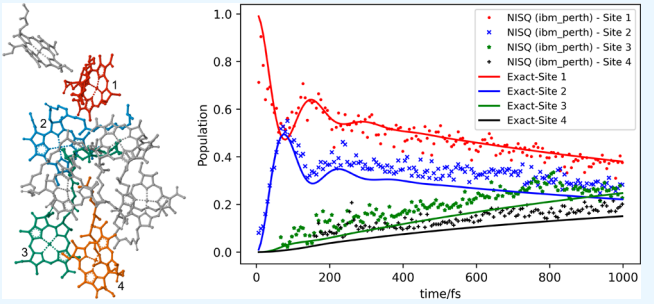

I. INTRODUCTION

Open quantum system dynamics has gained increasing research interest due to its direct applications to quantum dynamics in the condensed phase,[1−3] transport properties,[4,5] quantum biology,[6−8] and quantum error correction.[9] Recent advances have uncovered many intriguing phenomena, such as environment-assisted exciton transfer,[10−14] topological state preparation by reservoir engineering,[15,16] information backflow,[17,18] etc. Particularly for the non-Markovian bath, unique features exist, including coherence trapping,[19] enhanced quantum entanglement,[20] and the emergence of noncanonical equilibrium states.[21−23] Accurate and efficient modeling of non-Markovian quantum dynamics has important ramifications in chemistry for studying charge transfer reactions in solutions[24] and heterojunctions[25−27] as well as exciton transfer in macromolecules and molecular aggregates.[28,29] Due to the quantum mechanical nature of these processes, classical computer simulations can be prohibitively expensive due to the exponential scaling with the number of degrees of freedom and non-Markovianity.

Since the insightful suggestion by Feynman[30] and the pioneering demonstration by Lloyd,[31] numerous studies have emerged in seeking efficient quantum algorithms for quantum simulations.[32−38] As for open quantum systems, although a wealth of literature exists for Markovian dynamics, including the construction of a universal set of semigroup generators[39,40] and the development of various techniques for efficient Lindblad dynamics simulation,[41−51] quantum algorithms for non-Markovian evolution are much less explored and are still in the nascent stage of advancement. Notable studies include Sweke et al.[52] who considered locally indivisible maps that are capable of describing non-Markovian systems and Head-Marden et al.[53] who used ensembles of Lindblad trajectories originating from different times to capture the non-Markovian behavior. Wang et al.[54] constructed non-Markovian superoperators from the integrated generalized quantum master equation (GQME) and implemented them on NISQ devices through Sz.-Nagy dilation. Recently, a path integral based algorithm is proposed that encodes the Feynman−Vernon's influence functional on a quantum computer.[55]

The focus of this paper is to present a new quantum algorithm that captures the exact non-Markovian dynamics based on the construction of Kraus operators. We explicitly resort to Feynman's path integral formulation for generating the non-Markovian evolution. Adding to the existing pool of methods, our approach highlights two advantages. First, by implementing Kraus operators instead of superoperators on quantum machines, the propagation scheme is equivalent to

Received: December 5, 2023
Revised: January 18, 2024
Accepted: January 23, 2024
Published: February 15, 2024

time-evolving the wave function instead of the density matrix. As a consequence, it cuts the number of qubits needed by half. Second, by employing singular value decomposition (SVD), the nonunitary part is solely carried over to the diagonal matrix, which has efficient circuit implementation on quantum computers. These two merits lead to a shallow circuit structure that is amenable to simulating non-Markovian quantum dynamics using multiple qubits on NISQ devices. The organization of the paper is as follows. In Section II, we briefly review the operator-sum approach to open quantum system dynamics. In Section III, we describe the path integral techniques we use to construct exact non-Markovian super-propagators. In Section IV, we outline the procedures to construct Kraus operators from the superoperators. In Section V, we describe the unitarization of the Kraus operators using SVD and Walsh operators. In Section VI, we present simulation results on the NISQ device with two application cases, one based on the spin-boson model and the other based on the exciton transfer dynamics in the FMO complex. In Section VII, we offer concluding remarks.

II. OPERATOR-SUM APPROACH FOR OPEN QUANTUM SYSTEMS

The time evolution of the density matrix is described by

$$\rho(t) = U(t)\rho(0)U^{\dagger}(t) \tag{1}$$

where ρ refers to the total density matrix of the system and bath and $U(t)$ is the time evolution operator. In many cases, we are only interested in the dynamics of a subsystem, and the reduced dynamics is achieved by tracing out the environment's degrees of freedom. Without loss of generality, it is often assumed that the initial density matrix takes the tensor product form

$$\rho(0) = \rho_s(0) \otimes \rho_{env}(0) \tag{2}$$

Then, the reduced density matrix at time t is

$$\rho_s(t) = \mathrm{tr}_{env}[U(t)\rho_s(0) \otimes \rho_{env}(0)U^{\dagger}(t)] \tag{3}$$

$\rho_{env}(0)$ is expressed by its eigenstates

$$\rho_{env}(0) = \sum_i \lambda_i |\psi_i\rangle\langle\psi_i| \tag{4}$$

Equation 3 becomes

$$\rho_s(t) = \sum_j \sum_i \lambda_i \langle\psi_j|U(t)|\psi_i\rangle\rho_s(0)\langle\psi_i|U^{\dagger}(t)|\psi_j\rangle \tag{5}$$

Define

$$M_k(t) := \sqrt{\lambda_i}\langle\psi_j|U(t)|\psi_i\rangle \tag{6}$$

called the Kraus operator,[56] the reduced density matrix can be written as an operator-sum representation

$$\rho_s(t) = \sum_k M_k(t)\rho_s(0)M_k^{\dagger}(t) := \mathcal{E}_{t,0}(\rho_s(0)) \tag{7}$$

which defines a linear map $\mathcal{E}_{t,0}$ that is complete positive and trace-preserving (CPTP). It can be proven that for a subsystem spanning the Hilbert space of dimension d, at most d^2 numbers of Kraus operators are needed to completely mock up the CPTP map $\mathcal{E}_{t,0}$.[9]

The advantage of the Kraus operator representation is that the propagation scheme is analogous to the wave function propagation instead of the vectorized density matrix, therefore automatically reducing the number of qubits required by half and in turn shortening the circuit depth. Specifically, suppose $\rho_s(0)$ has the eigen decomposition $\rho_s(0) = \sum_i \sigma_i|\varphi_i\rangle\langle\varphi_i|$, then, the propagation can be achieved by each $M_k(t)|\varphi_i\rangle$. Notwithstanding the advantage, one major concern of its quantum computing implementation is that $M_k(t)$ is not unitary, and therefore, additional steps are required to convert it to a unitary operation. Schemes for converting nonunitary operators to unitary ones exist,[45,47,49,57−59] and in Section V, we will describe in detail the specific implementation used in this paper.

III. GENERATION OF THE LINEAR MAP $E_{t,0}$ FOR EXACT NON-MARKOVIAN DYNAMICS

We resort to the framework of a multistate system linearly coupled to its harmonic bath in the following discussion, for it has been shown to be widely applicable for simulating quantum dynamics in many condensed-phase systems.[3,24,25,28,60,61] In Feynman's path integral formulation,[62] the time evolution of the reduced density matrix has the form

$$\rho_s(s_t^+, s_t^-) = \int \mathcal{D}s^+ \int \mathcal{D}s^- \langle s_0^+|\rho_0(0)|s_0^-\rangle \exp\left\{\frac{i}{\hbar}(\mathcal{S}[s^+] - \mathcal{S}[s^-])\right\} IF[s^+, s^-] \tag{8}$$

where

$$IF[s^+, s^-] = \exp\left\{-\frac{1}{\hbar}\int_0^t \mathrm{d}t' \int_0^{t'} \mathrm{d}t''[s^+(t') - s^-(t')][\alpha(t' - t'')s^+(t'') - \alpha^*(t' - t'')s^-(t'')]\right\} \tag{9}$$

is Feynman−Vernon's influence functional,[63,64] with the s^+ and s^- being the forward and backward paths, respectively, $S[s^+]$ and $S[s^-]$ are the action integrals of the free system propagation, and $\langle s_0^+|\rho_0(0)|s_0^-\rangle$ is the initial state. The nonlocal memory kernel $\alpha(t' - t'')$ is the root of non-Markovianity and can be obtained from the bath response function

$$\alpha(t) = \frac{1}{\pi}\int_0^{\infty} \mathrm{d}\omega J(\omega)\left[\coth\left(\frac{\hbar\omega\beta}{2}\right)\cos(\omega t) - i\sin(\omega t)\right] \tag{10}$$

where the spectral density $J(\omega)$ is defined as

$$J(\omega) = \frac{\pi}{2}\sum_j \frac{c_j^2}{m_j\omega_j}\delta(\omega - \omega_j) \tag{11}$$

Here, ω_j is the collective mode of the bath and c_j is the coupling strength between the system and bath.

Equation 8 defines an exact linear map $\mathcal{E}_{t,0}$ for non-Markovian quantum dynamics of the subsystem. Several numerically efficient implementations are available, such as QuAPI,[65,66] QCPI,[67−69] SMatPI,[70−73] HEOM,[74−76] TEMPO,[77−79] TNPI,[80,81] etc. In this work, we use TNPI[80] to generate the linear map (i.e., the superoperator).

https://doi.org/10.1021/acsomega.3c09720
ACS Omega 2024, 9, 9666−9675

IV. FROM THE SUPEROPERATORS TO THE KRAUS OPERATORS

In this section, we outline the procedures for converting the superoperator to Kraus operators. By definition, a superoperator operates on a matrix, whereas an operator (or matrix) acts on a vector. It would be convenient to work in the matrix-vector scheme, and therefore, the initial step is to vectorize the density matrix, so that the superoperator can be expressed as a matrix. In this scheme, the superoperator acting on the density matrix can be written as

$$\mathrm{vec}(\rho(t)) = \mathcal{L}(t)\mathrm{vec}(\rho(0)) \tag{12}$$

where $\mathcal{L}(t)$ is the matrix representation of the linear map $\mathcal{E}_{t,0}$. The conversion of the superoperator $\mathcal{L}$ to an operator-sum representation relies on the construction of the Choi matrix[82,83] through the involution operation on $\mathcal{L}$, which is defined as

$$C := \sum_{i,j=1}^{N} (E_{i,j} \otimes I)\mathcal{L}(I \otimes E_{i,j}) \tag{13}$$

in which $E_{i,j}$ is a basis of an $N \times N$ matrix, with a "1" in the i, jth positions and zeros elsewhere. This Choi matrix is guaranteed to be positive and Hermitian for a CPTP map and therefore has an eigen decomposition with positive eigenvalues

$$C = \mathcal{U}\Sigma\mathcal{U}^{\dagger} = \sum_{k=1}^{N^2} \sigma_k u_k u_k^{\dagger} \tag{14}$$

The vectorized Kraus operator M_k is related to this decomposition by

$$\mathrm{vec}(M_k) = \sqrt{\sigma_k}\, u_k \tag{15}$$

Therefore, the matrix M_k can be reconstructed by taking the first N elements in $\boldsymbol{u}_k$ to be the first column, the $N + 1$ to $2N$ elements in $\boldsymbol{u}_k$ to be the second column, etc.

V. UNITARIZATION OF THE KRAUS OPERATORS

Useful schemes have been proposed to convert nonunitary operations into unitary ones that can be implemented on quantum computers. One is based on the block encoding in which the nonunitary part is embedded in a larger unitary matrix. The implementation involves ancilla qubits, and the measurement related to the nonunitary operator is usually nondeterministic. Common block-encoding schemes include Stinespring dilation,[58] Sz.-Nagy dilation,[59,84] quantum signal processing (QSP),[57,85,86] etc. Another popular scheme, called quantum imaginary time evolution (QITE),[49,50] is based on a mapping between a nonunitary operator and a parametrized unitary operator, in which the parameter is solved by an algebraic linear equation. In this paper, we unitarize the Kraus operator M_k through singular value decomposition (SVD). Specifically,

$$M_k = U\Sigma V^{\dagger} \tag{16}$$

where U and V are unitary matrices that can be directly implemented on a quantum computer. The $\sum$ matrix is a nonunitary diagonal and can be dilated to a unitary one in the following way.[47] First, a unitary operator associated with the elements of $\sum$ is defined by

$$U_{\Sigma} = \begin{pmatrix} \Sigma_{+} & 0 \\ 0 & \Sigma_{-} \end{pmatrix} \tag{17}$$

where

$$\Sigma_{\pm_j} = \sigma_j \pm i\sqrt{1 - \sigma_j^2} \tag{18}$$

with σ_j being the elements of $\sum$. It is worth mentioning that $|\sigma_j|$ is always smaller than 1, guaranteed by the fact that the CPTP map $\mathcal{E}_{t,0}$ is always contractive.[87] As the dilation is needed only for the diagonal instead of a general matrix, the circuit depth is expected to be short. Its advantage is further illustrated in Tables 1 and 2.

The circuit construction for the SVD[47] is shown in Figure 1, where the ancilla qubit implements the Hadamard gates.

The resulting states are

$$\frac{1}{2}\begin{pmatrix} U(\Sigma_{+} + \Sigma_{-})V^{\dagger}|\psi\rangle \\ U(\Sigma_{+} - \Sigma_{-})V^{\dagger}|\psi\rangle \end{pmatrix} = \begin{pmatrix} M_k|\psi\rangle \\ |\varphi\rangle \end{pmatrix} \tag{19}$$

in which the ancilla in the $|0\rangle$ state implements $M|\psi\rangle$, whereas the $|1\rangle$ state measurement (labeled $|\varphi\rangle$) is discarded. The measurement results show the statistics of $M_k|\psi\rangle\langle\psi|M_k^{\dagger}$ in the computational basis, which is exactly the element in the operator-sum representation in eq 7.

The diagonal unitary, eq 18, can be implemented efficiently on a quantum computer using the Walsh series representation.[88] Below, we summarize briefly the key construction. First, the integer j, $k \in [0, 2^{n-1}]$ is expressed in its binary and dyadic expansion, respectively

$$j = \sum_{i=1}^{n} j_i 2^{i-1} \tag{20}$$

$$k = \sum_{i=1}^{n} k_i 2^{n-i} \tag{21}$$

Table 1. Complexity Comparison of the Walsh Operator Approach vs Direct Compilation of the Diagonal Matrix for the 2 qubit and 3 qubit Problems in Section VI

	2 qubits		3 qubits	
	Walsh operator	direct compilation	Walsh operator	direct compilation
circuit depth	4	6	13	100
number of CNOT	2	2	9	35

Table 2. Complexity Comparison of SVD vs Sz.-Nagy Dilation for the 2 qubit and 3 qubit Problems in Section VI

	2 qubits		3 qubits	
	SVD	Sz.-Nagy dilation	SVD	Sz.-Nagy dilation
circuit depth	11	14	46	123
number of CNOT	2	2	15	36

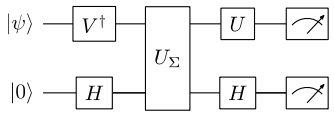

Figure 1. Circuit for SVD.

https://doi.org/10.1021/acsomega.3c09720
ACS Omega 2024, 9, 9666−9675

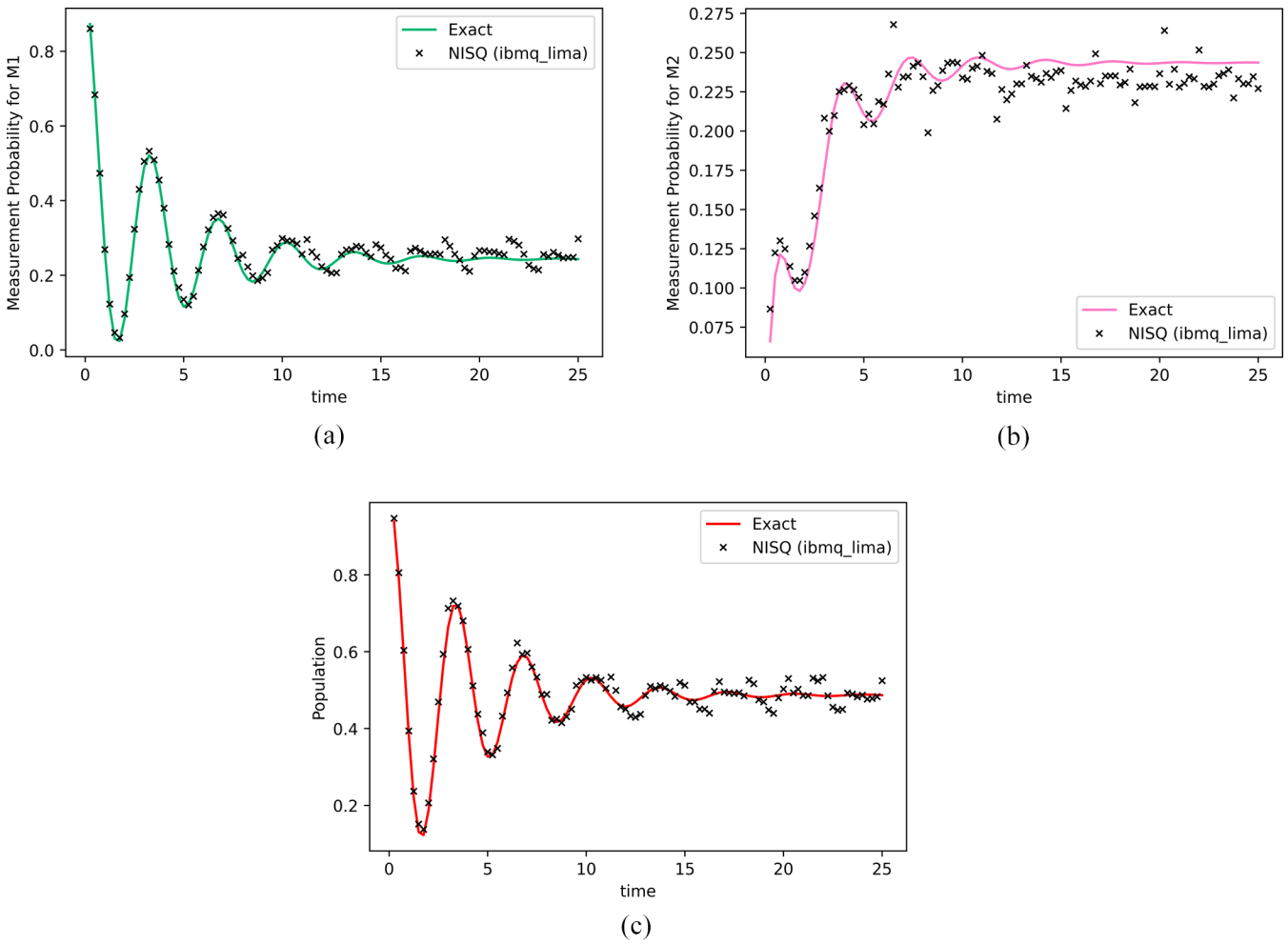

Figure 2. (a, b) Measurement results for the non-zero Kraus operators M_k and (c) population dynamics with parameters $\Omega = 1$, $\epsilon = 0$, $\xi = 0.1$, $\omega_c = 7.5$, and $\beta = 5$. (The time is in atomic unit.) The crosses are the results from *ibm_lima*, and the curves are the exact results. Each time point is obtained by 20,000 shots.

where n is the number of qubits required to implement eq 17.

A matrix W_{jk} and a vector f_k are defined as

$$W_{jk} = (-1)^{\sum_{i=1}^{n} j_i k_i} \tag{22}$$

$$f_k = (\ln U_\Sigma)_k \tag{23}$$

The Walsh coefficient a_j is obtained from the Walsh–Fourier transform of f_k

$$a_j = \frac{1}{2^n} \sum_{k=1}^{2^n} W_{jk} f_k \tag{24}$$

Then, the unitary diagonal U_Σ can be expressed as

$$U_\Sigma = \prod_{j=1}^{2^n} e^{i a_j \hat{Q}_j} \tag{25}$$

with the Walsh operator $\hat{Q}_j$ given as the tensor product of Pauli Z gates

$$\hat{Q}_j = (\sigma_{z_1})^{j_1} \otimes (\sigma_{z_2})^{j_2} \otimes \cdots \otimes (\sigma_{z_n})^{j_n} \tag{26}$$

The circuit for the exponentiation of the tensor product of Pauli gates can be constructed[9] and further optimized[88,89] with the Gray code ordering to minimize the number of CNOT gates.

To validate the effectiveness of the Walsh series approach, we compare the gate complexity (circuit depth and the gate counts) using the optimal Walsh operators with that of the direct compilation of the unitary diagonal on Qiskit,[90] all decomposed to the native gate sets of X, $\sqrt{X}$, R_Z, and CNOT and complied to the topology of *ibm_perth* (shown in Figure S1). Table 1 gives the summary, and the circuits are shown in the Supporting Information (SI), Figures S2–S5.

We also compare the gate complexity of using SVD for unitarization of the Kraus operator to that of Sz.-Nagy dilation, compiled to the *ibm_perth* topology, and the results are shown in Table 2. The circuits are given in the SI, Figures S6–S9.

From a more quantitative perspective, for an n qubit problem, the number of single and CNOT gates scales as $O(n^2 4^n)$,[9] which is the cost of Sz.-Nagy dilation. In the SVD approach, only the diagonal needs to be dilated, and the compilation of the two unitary matrices involves one qubit less and therefore only scales as $O((n-1)^2 4^{(n-1)})$. The dilated diagonal with the Walsh operator implementation scales at most $O(2^n)$.[88] Therefore, it is no surprise that the SVD plus Walsh operator approach outperforms the Sz.-Nagy dilation.

https://doi.org/10.1021/acsomega.3c09720
ACS Omega 2024, 9, 9666−9675

VI. RESULTS AND DISCUSSION

VI.I. Two-Level System. In this subsection, we present the simulation results for the spin-boson model,[63] with the system-bath Hamiltonian given by

$$H = -\hbar\sigma_x + \hbar\varepsilon\sigma_z + \sum_j \left[\frac{p_j^2}{2m_j} + \frac{1}{2}m_j\omega_j^2\left(Q_j - \frac{c_j\sigma_z}{m_j\omega_j^2}\right)^2\right] \tag{27}$$

We choose the spectral density to have the Ohmic form

$$J(\omega) = \frac{\pi}{2}\hbar\xi\omega e^{-\omega/\omega_c} \tag{28}$$

which gives a continuous version of eq 11. It is worth mentioning that for a real molecular environment with discrete modes that resemble the ohmic form, the discretization of eq 28 gives a direct relationship between ξ, ω_c and c_j, and ω_j in eq 27.[91,92] In our simulation, the system bath parameters are with the following: tunneling frequency Ω = 1, asymmetry ϵ = 0, coupling strength ξ = 0.1, cutoff frequency ω_c = 7.5, and inverse temperature β = 5. In this parameter regime, we observe that out of the four Kraus operators, only two are significantly contributing. Figure 2a,b shows the measurement results for each of the two Kraus operators on the IBM NISQ device, and Figure 2c shows the population dynamics when adding them together. The NISQ results match well with the exact calculation from TNPI.[80]

VI.II. Exciton Dynamics for FMO. The FMO complex and its functional subsystems have received intense research investigation[93−98] regarding its light harvesting efficiency and the quantum mechanical nature of the exciton transport. In this subsection, we study the exciton transfer dynamics in a major pathway 1 → 2 → 3 → 4 of the FMO, shown in Figure 3.

For this 4-site model, the Hamiltonian has the following Frenkel−Holstein[99−101] form

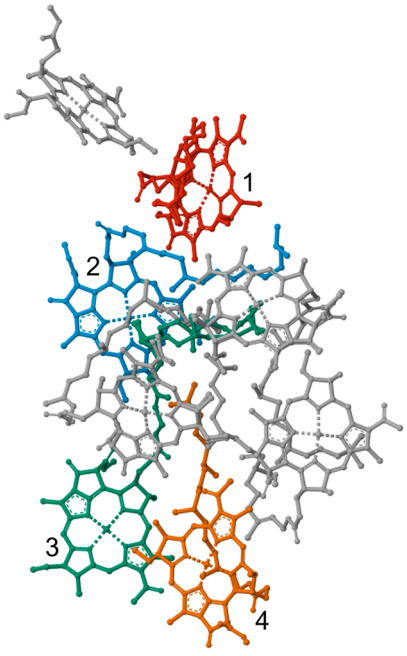

Figure 3. FMO complex and major pathway 1 → 2 → 3 → 4.

$$H = \sum_{k=1}^{4} \epsilon_k|k\rangle\langle k| + \sum_{j\neq k} h_{j.k}|j\rangle\langle k| + \sum_{k=1}^{4}\sum_{j=1}^{N_{occ}}\left[\frac{p_{kj}^2}{2m_{kj}} + \frac{1}{2}m_{kj}\omega_{kj}^2\left(x_{kj} - \frac{c_{kj}|k\rangle\langle k|}{m_{kj}\omega_{kj}^2}\right)^2\right] \tag{29}$$

The system Hamiltonian is taken from the work done by Read et al.[102] (see more details in SI eq (S.1))

$$H_0 = \begin{pmatrix} 12\,375 & -87.7 & 5.5 & -5.9 \\ -87.7 & 12\,495 & 30.8 & 8.2 \\ 5.5 & 30.8 & 12\,175 & -53.4 \\ -5.9 & 8.2 & -53.5 & 12\,285 \end{pmatrix} \tag{30}$$

The values are in units of cm^{-1}. Each exciton is coupled to its local harmonic bath that assumes the same Drude spectral density

$$J(\omega) = \frac{2\lambda\gamma\omega}{\omega^2 + \gamma^2} \tag{31}$$

with the reorganization energy λ = 35 cm^{-1} and phonon relaxation rate γ = 106.18 cm^{-1}.[103] The temperature of the simulation is 300 K.

Among all 16 Kraus operators, only a handful are significantly contributing. Figure 4a−f shows some representative Kraus operator measurement results on the IBM NISQ device. With two qubits (plus one ancilla) representing the four sites, each Kraus operator has four measurement probabilities, labeled 00, 01, 10, and 00 in the Qiskit convention. It is not entirely clear to us why the Kraus operators have jumps at specific times. However, these discontinuous jumps cancel each other and produce smooth dynamics when adding them together. Figure 5a,b shows the population dynamics of the four sites by adding all the individual Kraus operators, with (a) being the simulator results and (b) being the real device. The NISQ results show quantitative agreement with the exact solution.

VII. CONCLUSIONS

We have demonstrated a feasible quantum algorithm for simulating exact non-Markovian dynamics on the NISQ device. The shallow circuit is achieved by three strategies. First, instead of implementing the superoperator directly, we choose to implement its associated Kraus operators. This is equivalent to propagating the wave function instead of the vectorized density matrix. Reducing the dimensionality from n^2 to n, where n is the size of the wavevector, it automatically saves half of the qubits and as a consequence shrinks the circuit depth. Second, we employ SVD to encode the nonunitary Kraus operators. With two unitary matrices naturally coming out of this procedure, the dilation is only applied to the diagonal part. Third, we employ the optimal Walsh operators to implement the unitary diagonal. The combination of the SVD and the Walsh operator approach results in significant improvement in compilation complexity compared to the Sz.-Nagy dilation. As a general figure of merit for the above numerically exact algorithm, the number of nonzero Kraus operators often does not grow exponentially with the system size, therefore circumventing the costly measurement overhead. With respect to the spectral density, this theoretical framework allows an arbitrary form. In conclusion,

https://doi.org/10.1021/acsomega.3c09720
ACS Omega 2024, 9, 9666−9675

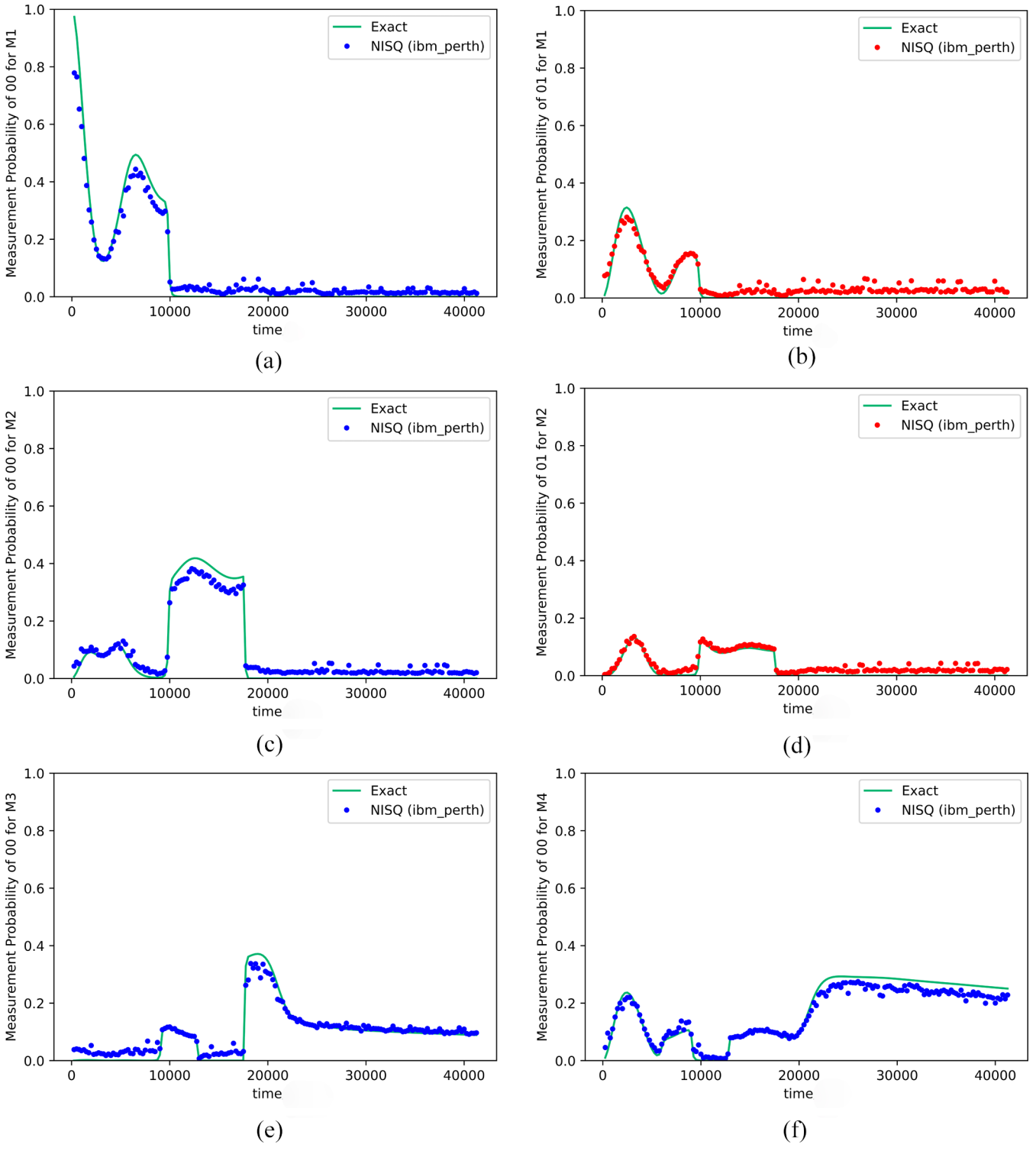

Figure 4. (a–f) Measurement results for the representative Kraus operators M_k for the FMO. The system Hamiltonian is taken from ref 84 and the bath parameters are λ = 35 cm^{-1} and γ = 106.18 cm^{-1} for the Drude spectral density[103] and the temperature is 300 K. (The time is in atomic unit.) The dots are the results from *ibm_perth*, and the curves are the exact results. Each time point is obtained by 50,000 shots.

the successful implementation on the NISQ device with the 4-site model suggests that the algorithm can potentially handle even larger Hilbert space (more qubits) without incurring too much noise.

■ ASSOCIATED CONTENT

Supporting Information

The Supporting Information is available free of charge at https://pubs.acs.org/doi/10.1021/acsomega.3c09720.

Topology of *ibm_perth*, compiled circuits on *ibm_perth* for the diagonal matrix as well as the Kraus operators for the two-level and the four-site model, using both the

https://doi.org/10.1021/acsomega.3c09720
ACS Omega 2024, 9, 9666−9675

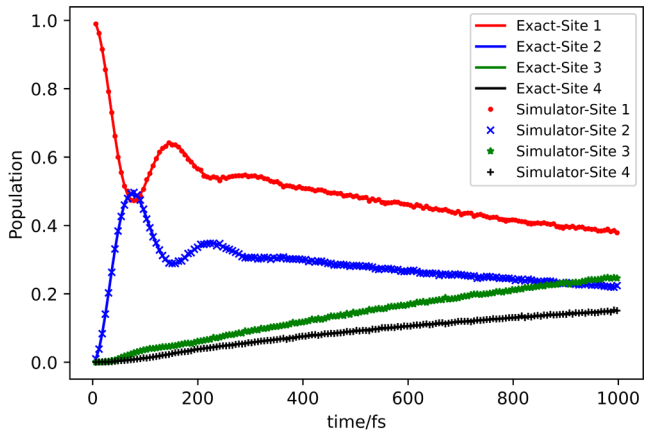

Figure 5. Population dynamics for a major pathway 1 → 2 → 3 → 4 in FMO on (a) simulators and (b) IBM device, with crosses representing the results from *ibmq_perth*. (The time unit is given in fs).

singular value decomposition and direct compilation methods, and four-site system Hamiltonian values explained (PDF)

AUTHOR INFORMATION

Corresponding Author

Fei Wang − *Department of Chemistry and Biochemistry and Quantum Science and Engineering Center, George Mason University, Fairfax, Virginia 22030, United States;* orcid.org/0000-0003-2233-4741; Email: fwang22@gmu.edu

Authors

Avin Seneviratne − *Department of Physics and Astronomy, George Mason University, Fairfax, Virginia 22030, United States*

Peter L. Walters − *Department of Chemistry and Biochemistry, George Mason University, Fairfax, Virginia 22030, United States*

Complete contact information is available at: https://pubs.acs.org/10.1021/acsomega.3c09720

Notes

The authors declare no competing financial interest.

ACKNOWLEDGMENTS

This work was supported by National Science Foundation (NSF) under Award 2320328 and George Mason University's startup fund and its Science and Engineering Center (QSEC) funding. The authors acknowledge the use of IBM Quantum services for this work. The views expressed are those of the authors and do not reflect the official policy or position of IBM or the IBM Quantum team.

REFERENCES

(1) Breuer, H.-P.; Petruccione, F. *The Theory of Open Quantum Systems*; Clarendon Press: Oxford, 2010.
(2) Weiss, U. *Quantum Dissipative Systems*, 4th ed.; World Scientific, 2012.
(3) Nitzan, A. *Chemical Dynamics in Condensed Phases: Relaxation, Transfer and Reactions in Condensed Molecular Systems*; Oxford University Press: Oxford, 2013.
(4) Bose, A.; Walters, P. L. Effect of Temperature Gradient on Quantum Transport. *Phys. Chem. Chem. Phys.* **2022**, *24* (37), 22431−22436.
(5) Bose, A.; Walters, P. L. Impact of Solvent on State-to-State Population Transport in Multistate Systems Using Coherences. *J. Chem. Theory Comput.* **2023**, *19* (15), 4828−4836.
(6) Lambert, N.; Chen, Y.-N.; Cheng, Y.-C.; Li, C.-M.; Chen, G.-Y.; Nori, F. Quantum Biology. *Nat. Phys.* **2013**, *9* (1), 10−18.
(7) Mohseni, M.; Omar, Y.; Engel, G.; Plenio, M. B. *Quantum Effects in Biology*; Cambridge University Press: Cambridge, 2014.
(8) Cao, J.; Cogdell, R. J.; Coker, D. F.; Duan, H.-G.; Hauer, J.; Kleinekathöfer, U.; Jansen, T. L. C.; Mančal, T.; Miller, R. J. D.; Ogilvie, J. P.; Prokhorenko, V. I.; Renger, T.; Tan, H.-S.; Tempelaar, R.; Thorwart, M.; Thyrhaug, E.; Westenhoff, S.; Zigmantas, D. Quantum Biology Revisited. *Sci. Adv.* **2020**, *6* (14), No. eaaz4888.
(9) Nielsen, M. A.; Chuang, I. L. *Quantum Computation and Quantum Information: 10th Anniversary ed.*, 1st ed.; Cambridge University Press, 2012.
(10) Mohseni, M.; Rebentrost, P.; Lloyd, S.; Aspuru-Guzik, A. Environment-Assisted Quantum Walks in Photosynthetic Energy Transfer. *J. Chem. Phys.* **2008**, *129* (17), No. 174106.
(11) Rebentrost, P.; Mohseni, M.; Kassal, I.; Lloyd, S.; Aspuru-Guzik, A. Environment-Assisted Quantum Transport. *New J. Phys.* **2009**, *11* (3), No. 033003.
(12) Chin, A. W.; Datta, A.; Caruso, F.; Huelga, S. F.; Plenio, M. B. Noise-Assisted Energy Transfer in Quantum Networks and Light-Harvesting Complexes. *New J. Phys.* **2010**, *12* (6), No. 065002.
(13) Kassal, I.; Aspuru-Guzik, A. Environment-Assisted Quantum Transport in Ordered Systems. *New J. Phys.* **2012**, *14* (5), No. 053041.
(14) Zerah-Harush, E.; Dubi, Y. Universal Origin for Environment-Assisted Quantum Transport in Exciton Transfer Networks. *J. Phys. Chem. Lett.* **2018**, *9* (7), 1689−1695.
(15) Diehl, S.; Rico, E.; Baranov, M. A.; Zoller, P. Topology by Dissipation in Atomic Quantum Wires. *Nat. Phys.* **2011**, *7* (12), 971−977.
(16) Bardyn, C.-E.; Baranov, M. A.; Kraus, C. V.; Rico, E.; İmamoğlu, A.; Zoller, P.; Diehl, S. Topology by Dissipation. *New J. Phys.* **2013**, *15* (8), No. 085001.
(17) Breuer, H.-P.; Laine, E.-M.; Piilo, J. Measure for the Degree of Non-Markovian Behavior of Quantum Processes in Open Systems. *Phys. Rev. Lett.* **2009**, *103* (21), No. 210401.
(18) Bylicka, B.; Chruściński, D.; Maniscalco, S. Non-Markovianity and Reservoir Memory of Quantum Channels: A Quantum Information Theory Perspective. *Sci. Rep.* **2014**, *4* (1), No. 5720.
(19) Addis, C.; Brebner, G.; Haikka, P.; Maniscalco, S. Coherence Trapping and Information Backflow in Dephasing Qubits. *Phys. Rev. A* **2014**, *89* (2), No. 024101.
(20) Thorwart, M.; Eckel, J.; Reina, J. H.; Nalbach, P.; Weiss, S. Enhanced Quantum Entanglement in the Non-Markovian Dynamics

https://doi.org/10.1021/acsomega.3c09720
ACS Omega 2024, 9, 9666−9675

of Biomolecular Excitons. *Chem. Phys. Lett.* **2009**, *478* (4−6), 234−237.
(21) Cai, C. Y.; Yang, L.-P.; Sun, C. P. Threshold for Nonthermal Stabilization of Open Quantum Systems. *Phys. Rev. A* **2014**, *89* (1), No. 012128.
(22) Iles-Smith, J.; Lambert, N.; Nazir, A. Environmental Dynamics, Correlations, and the Emergence of Noncanonical Equilibrium States in Open Quantum Systems. *Phys. Rev. A* **2014**, *90* (3), No. 032114.
(23) Spaventa, G.; Huelga, S. F.; Plenio, M. B. Capacity of Non-Markovianity to Boost the Efficiency of Molecular Switches. *Phys. Rev. A* **2022**, *105* (1), No. 012420.
(24) Walters, P. L.; Makri, N. Quantum−Classical Path Integral Simulation of Ferrocene−Ferrocenium Charge Transfer in Liquid Hexane. *J. Phys. Chem. Lett.* **2015**, *6* (24), 4959−4965.
(25) Tamura, H.; Martinazzo, R.; Ruckenbauer, M.; Burghardt, I. Quantum Dynamics of Ultrafast Charge Transfer at an Oligothiophene-Fullerene Heterojunction. *J. Chem. Phys.* **2012**, *137* (22), No. 22A540.
(26) Binder, R.; Lauvergnat, D.; Burghardt, I. Conformational Dynamics Guides Coherent Exciton Migration in Conjugated Polymer Materials: First-Principles Quantum Dynamical Study. *Phys. Rev. Lett.* **2018**, *120* (22), No. 227401.
(27) Tamura, H.; Bittner, E. R.; Burghardt, I. Exciton Dissociation at Donor-Acceptor Polymer Heterojunctions: Quantum Nonadiabatic Dynamics and Effective-Mode Analysis. *J. Chem. Phys.* **2007**, *126* (2), No. 021103.
(28) Kundu, S.; Makri, N. Exciton−Vibration Dynamics in J-Aggregates of a Perylene Bisimide from Real-Time Path Integral Calculations. *J. Phys. Chem. C* **2021**, *125* (1), 201−210.
(29) Kundu, S.; Dani, R.; Makri, N. Tight Inner Ring Architecture and Quantum Motion of Nuclei Enable Efficient Energy Transfer in Bacterial Light Harvesting. *Sci. Adv.* **2022**, *8* (43), No. eadd0023.
(30) Feynman, R. P. Simulating Physics with Computers. *Int. J. Theor. Phys.* **1982**, *21* (6−7), 467−488.
(31) Lloyd, S. Universal Quantum Simulators. *Science* **1996**, *273* (5278), 1073−1078.
(32) Berry, D. W.; Ahokas, G.; Cleve, R.; Sanders, B. C. Efficient Quantum Algorithms for Simulating Sparse Hamiltonians. *Commun. Math. Phys.* **2007**, *270* (2), 359−371.
(33) Barison, S.; Vicentini, F.; Carleo, G. An Efficient Quantum Algorithm for the Time Evolution of Parameterized Circuits. *Quantum* **2021**, *5*, No. 512.
(34) Li, Y.; Benjamin, S. C. Efficient Variational Quantum Simulator Incorporating Active Error Minimization. *Phys. Rev. X* **2017**, *7* (2), No. 021050.
(35) Daley, A. J.; Bloch, I.; Kokail, C.; Flannigan, S.; Pearson, N.; Troyer, M.; Zoller, P. Practical Quantum Advantage in Quantum Simulation. *Nature* **2022**, *607* (7920), 667−676.
(36) Berry, D. W.; Childs, A. M.; Cleve, R.; Kothari, R.; Somma, R. D. Simulating Hamiltonian Dynamics with a Truncated Taylor Series. *Phys. Rev. Lett.* **2015**, *114* (9), No. 090502.
(37) Campbell, E. Random Compiler for Fast Hamiltonian Simulation. *Phys. Rev. Lett.* **2019**, *123* (7), No. 070503.
(38) Cîrstoiu, C.; Holmes, Z.; Iosue, J.; Cincio, L.; Coles, P. J.; Sornborger, A. Variational Fast Forwarding for Quantum Simulation beyond the Coherence Time. *npj Quantum Inf.* **2020**, *6* (1), No. 82.
(39) Bacon, D.; Childs, A. M.; Chuang, I. L.; Kempe, J.; Leung, D. W.; Zhou, X. Universal Simulation of Markovian Quantum Dynamics. *Phys. Rev. A* **2001**, *64* (6), No. 062302.
(40) Sweke, R.; Sinayskiy, I.; Bernard, D.; Petruccione, F. Universal Simulation of Markovian Open Quantum Systems. *Phys. Rev. A* **2015**, *91* (6), No. 062308.
(41) Childs, A. M.; Li, T. Efficient Simulation of Sparse Markovian Quantum Dynamics **2017**, arXiv:1611.05543. arXiv.org e-Printarchive. https://arxiv.org/abs/1611.0554.
(42) Cleve, R.; Wang, C. Efficient Quantum Algorithms for Simulating Lindblad Evolution **2016**, arXiv:1612.09512. arXiv.org e-Printarchive. https://arxiv.org/abs/1612.09512.
(43) Hu, Z.; Xia, R.; Kais, S. A Quantum Algorithm for Evolving Open Quantum Dynamics on Quantum Computing Devices. *Sci. Rep.* **2020**, *10* (1), No. 3301.
(44) Hu, Z.; Head-Marsden, K.; Mazziotti, D. A.; Narang, P.; Kais, S. A General Quantum Algorithm for Open Quantum Dynamics Demonstrated with the Fenna-Matthews-Olson Complex. *Quantum* **2022**, *6*, No. 726.
(45) Schlimgen, A. W.; Head-Marsden, K.; Sager, L. M.; Narang, P.; Mazziotti, D. A. Quantum Simulation of Open Quantum Systems Using a Unitary Decomposition of Operators. *Phys. Rev. Lett.* **2021**, *127* (27), No. 270503.
(46) Schlimgen, A. W.; Head-Marsden, K.; Sager-Smith, L. M.; Narang, P.; Mazziotti, D. A. Quantum Simulation of Open Quantum Systems Using Density-Matrix Purification **2022**, arXiv:2207.07112. arXiv.org e-Printarchive. https://arxiv.org/abs/2207.07112.
(47) Schlimgen, A. W.; Head-Marsden, K.; Sager-Smith, L. M.; Narang, P.; Mazziotti, D. A. Quantum State Preparation and Nonunitary Evolution with Diagonal Operators. *Phys. Rev. A* **2022**, *106* (2), No. 022414.
(48) Endo, S.; Sun, J.; Li, Y.; Benjamin, S. C.; Yuan, X. Variational Quantum Simulation of General Processes. *Phys. Rev. Lett.* **2020**, *125* (1), No. 010501.
(49) Kamakari, H.; Sun, S.-N.; Motta, M.; Minnich, A. J. Digital Quantum Simulation of Open Quantum Systems Using Quantum Imaginary−Time Evolution. *PRX Quantum* **2022**, *3* (1), No. 010320.
(50) Motta, M.; Sun, C.; Tan, A. T. K.; O'Rourke, M. J.; Ye, E.; Minnich, A. J.; Brandão, F. G. S. L.; Chan, G. K.-L. Determining Eigenstates and Thermal States on a Quantum Computer Using Quantum Imaginary Time Evolution. *Nat. Phys.* **2020**, *16* (2), 205−210.
(51) Chan, H. H. S.; Ramo, D. M.; Fitzpatrick, N. Simulating Non-Unitary Dynamics Using Quantum Signal Processing with Unitary Block Encoding **2023**, arXiv:2303.06161. arXiv.org e-Printarchive. https://arxiv.org/abs/2303.06161.
(52) Sweke, R.; Sanz, M.; Sinayskiy, I.; Petruccione, F.; Solano, E. Digital Quantum Simulation of Many-Body Non-Markovian Dynamics. *Phys. Rev. A* **2016**, *94* (2), No. 022317.
(53) Head-Marsden, K.; Krastanov, S.; Mazziotti, D. A.; Narang, P. Capturing Non-Markovian Dynamics on near-Term Quantum Computers. *Phys. Rev. Res.* **2021**, *3* (1), No. 013182.
(54) Wang, Y.; Mulvihill, E.; Hu, Z.; Lyu, N.; Shivpuje, S.; Liu, Y.; Soley, M. B.; Geva, E.; Batista, V. S.; Kais, S. Simulating Open Quantum System Dynamics on NISQ Computers with Generalized Quantum Master Equations. *J. Chem. Theory Comput.* **2023**, *19* (15), 4851−4862.
(55) Walters, P. L.; Wang, F. Path integral quantum algorithm for simulating non-Markovian quantum dynamics in open quantum systems. *Phys. Rev. Res.* **2024**, *6*, 13135.
(56) States, Effects, and Operations Fundamental Notions of Quantum Theory. In *Lecture Notes in Physics*; Kraus, K.; Böhm, A.; Dollard, J. D.; Wootters, W. H., Eds.; Springer Berlin Heidelberg: Berlin, Heidelberg, 1983; Vol. *190*.
(57) Martyn, J. M.; Rossi, Z. M.; Tan, A. K.; Chuang, I. L. Grand Unification of Quantum Algorithms. *PRX Quantum* **2021**, *2* (4), No. 040203.
(58) Stinespring, W. F. Positive Functions on C * -Algebras. *Proc. Am. Math. Soc.* **1955**, *6* (2), 211−216.
(59) Paulsen, V. *Completely Bounded Maps and Operator Algebras*, 1st ed.; Cambridge University Press, 2003.
(60) Klymko, K.; Mejuto-Zaera, C.; Cotton, S. J.; Wudarski, F.; Urbanek, M.; Hait, D.; Head-Gordon, M.; Whaley, K. B.; Moussa, J.; Wiebe, N.; de Jong, W. A.; Tubman, N. M. Real-Time Evolution for Ultracompact Hamiltonian Eigenstates on Quantum Hardware. *PRX Quantum* **2022**, *3* (2), No. 020323.
(61) Kundu, S.; Dani, R.; Makri, N. B800-to-B850 Relaxation of Excitation Energy in Bacterial Light Harvesting: All-State, All-Mode Path Integral Simulations. *J. Chem. Phys.* **2022**, *157* (1), No. 015101.
(62) Feynman, R. P. Space-Time Approach to Non-Relativistic Quantum Mechanics. *Rev. Mod. Phys.* **1948**, *20* (2), 367−387.

https://doi.org/10.1021/acsomega.3c09720
ACS Omega 2024, 9, 9666−9675

(63) Leggett, A. J.; Chakravarty, S.; Dorsey, A. T.; Fisher, M. P. A.; Garg, A.; Zwerger, W. Dynamics of the Dissipative Two-State System. *Rev. Mod. Phys.* **1987**, *59* (1), 1−85.
(64) Feynman, R. P.; Vernon, F. L. The Theory of a General Quantum System Interacting with a Linear Dissipative System. *Ann. Phys.* **1963**, *24*, 118−173.
(65) Topaler, M.; Makri, N. System-Specific Discrete Variable Representations for Path Integral Calculations with Quasi-Adiabatic Propagators. *Chem. Phys. Lett.* **1993**, *210* (4−6), 448−457.
(66) Makri, N. Numerical Path Integral Techniques for Long Time Dynamics of Quantum Dissipative Systems. *J. Math. Phys.* **1995**, *36* (5), 2430−2457.
(67) Lambert, R.; Makri, N. Quantum-Classical Path Integral. I. Classical Memory and Weak Quantum Nonlocality. *J. Chem. Phys.* **2012**, *137* (22), No. 22A552.
(68) Lambert, R.; Makri, N. Quantum-Classical Path Integral. II. Numerical Methodology. *J. Chem. Phys.* **2012**, *137* (22), No. 22A553.
(69) Wang, F.; Makri, N. Quantum-Classical Path Integral with a Harmonic Treatment of the Back-Reaction. *J. Chem. Phys.* **2019**, *150* (18), No. 184102.
(70) Makri, N. Small Matrix Path Integral for System-Bath Dynamics. *J. Chem. Theory Comput.* **2020**, *16* (7), 4038−4049.
(71) Makri, N. Small Matrix Disentanglement of the Path Integral: Overcoming the Exponential Tensor Scaling with Memory Length. *J. Chem. Phys.* **2020**, *152* (4), No. 041104.
(72) Makri, N. Small Matrix Path Integral for Driven Dissipative Dynamics. *J. Phys. Chem. A* **2021**, *125* (48), 10500−10506.
(73) Makri, N. Small Matrix Decomposition of Feynman Path Amplitudes. *J. Chem. Theory Comput.* **2021**, *17* (7), 3825−3829.
(74) Tanimura, Y. Numerically "Exact" Approach to Open Quantum Dynamics: The Hierarchical Equations of Motion (HEOM). *J. Chem. Phys.* **2020**, *153* (2), No. 020901.
(75) Tanimura, Y. Reduced Hierarchical Equations of Motion in Real and Imaginary Time: Correlated Initial States and Thermodynamic Quantities. *J. Chem. Phys.* **2014**, *141* (4), No. 044114.
(76) Tanimura, Y. Real-Time and Imaginary-Time Quantum Hierarchal Fokker-Planck Equations. *J. Chem. Phys.* **2015**, *142* (14), No. 144110.
(77) Strathearn, A.; Kirton, P.; Kilda, D.; Keeling, J.; Lovett, B. W. Efficient Non-Markovian Quantum Dynamics Using Time-Evolving Matrix Product Operators. *Nat. Commun.* **2018**, *9* (1), No. 3322.
(78) Jørgensen, M. R.; Pollock, F. A. Exploiting the Causal Tensor Network Structure of Quantum Processes to Efficiently Simulate Non-Markovian Path Integrals. *Phys. Rev. Lett.* **2019**, *123* (24), No. 240602.
(79) Richter, M.; Hughes, S. Enhanced TEMPO Algorithm for Quantum Path Integrals with Off-Diagonal System-Bath Coupling: Applications to Photonic Quantum Networks. *Phys. Rev. Lett.* **2022**, *128* (16), No. 167403.
(80) Bose, A.; Walters, P. L. A Tensor Network Representation of Path Integrals: Implementation and Analysis **2021**, arXiv:2106.12523. arXiv.org e-Printarchive. https://arxiv.org/abs/2106.12523.
(81) Bose, A.; Walters, P. L. A Multisite Decomposition of the Tensor Network Path Integrals. *J. Chem. Phys.* **2022**, *156* (2), No. 024101.
(82) Havel, T. F. Robust Procedures for Converting among Lindblad, Kraus and Matrix Representations of Quantum Dynamical Semigroups. *J. Math. Phys.* **2003**, *44* (2), 534−557.
(83) Choi, M.-D. Completely Positive Linear Maps on Complex Matrices. *Linear Algebra Appl.* **1975**, *10* (3), 285−290.
(84) Schäffer, J. J. On Unitary Dilations of Contractions. *Proc. Am. Math. Soc.* **1955**, *6* (2), No. 322.
(85) Low, G. H.; Chuang, I. L. Optimal Hamiltonian Simulation by Quantum Signal Processing. *Phys. Rev. Lett.* **2017**, *118* (1), No. 010501.
(86) Gilyén, A.; Su, Y.; Low, G. H.; Wiebe, N. In *Quantum Singular Value Transformation and beyond: Exponential Improvements for Quantum Matrix Arithmetics*, Proceedings of the 51st Annual ACM SIGACT Symposium on Theory of Computing; ACM: Phoenix AZ USA, 2019; pp 193−204.
(87) Rivas, Á.; Huelga, S. F.; Plenio, M. B. Quantum Non-Markovianity: Characterization, Quantification and Detection. *Rep. Prog. Phys.* **2014**, *77* (9), No. 094001.
(88) Welch, J.; Greenbaum, D.; Mostame, S.; Aspuru-Guzik, A. Efficient Quantum Circuits for Diagonal Unitaries without Ancillas. *New J. Phys.* **2014**, *16* (3), No. 033040.
(89) Bullock, S. S.; Markov, I. L. Smaller Circuits for Arbitrary N-Qubit Diagonal Computations **2003**, arXiv:quant-ph/0303039. arXiv.org e-Printarchive. https://arxiv.org/abs/quant-ph/0303039.
(90) Aleksandrowicz, G.; Alexander, T.; Barkoutsos, P.; Bello, L.; Ben-Haim, Y.; Bucher, D.; Cabrera-Hernández, F. J.; Carballo-Franquis, J.; Chen, A.; Chen, C.-F.; Chow, J. M.; Córcoles-Gonzales, A. D.; Cross, A. J.; Cross, A.; Cruz-Benito, J.; Culver, C.; De La Puente González, S.; De La Torre, E.; Ding, D.; Dumitrescu, E.; Duran, I.; Eendebak, P.; Everitt, M.; Sertage, I. F.; Frisch, A.; Fuhrer, A.; Gambetta, J.; Gago, B. G.; Gomez-Mosquera, J.; Greenberg, D.; Hamamura, I.; Havlicek, V.; Hellmers, J.; Herok, L.; Horii, H.; Hu, S.; Imamichi, T.; Itoko, T.; Javadi-Abhari, A.; Kanazawa, N.; Karazeev, A.; Krsulich, K.; Liu, P.; Luh, Y.; Maeng, Y.; Marques, M.; Martín-Fernández, F. J.; McClure, D. T.; McKay, D.; Meesala, S.; Mezzacapo, A.; Moll, N.; Rodríguez, D. M.; Nannicini, G.; Nation, P.; Ollitrault, P.; O'Riordan, L. J.; Paik, H.; Pérez, J.; Phan, A.; Pistoia, M.; Prutyanov, V.; Reuter, M.; Rice, J.; Davila, A. R.; Rudy, R. H. P.; Ryu, M.; Sathaye, N.; Schnabel, C.; Schoute, E.; Setia, K.; Shi, Y.; Silva, A.; Siraichi, Y.; Sivarajah, S.; Smolin, J. A.; Soeken, M.; Takahashi, H.; Tavernelli, I.; Taylor, C.; Taylour, P.; Trabing, K.; Treinish, M.; Turner, W.; Vogt-Lee, D.; Vuillot, C.; Wildstrom, J. A.; Wilson, J.; Winston, E.; Wood, C.; Wood, S.; Wörner, S.; Akhalwaya, I. Y.; Zoufal, C.*Qiskit: An Open-Source Framework for Quantum Computing*, Version 0.7.2; Zenodo, 2019 DOI: 10.5281/ZENODO.2562110.
(91) Makri, N. The Linear Response Approximation and Its Lowest Order Corrections: An Influence Functional Approach. *J. Phys. Chem. B* **1999**, *103* (15), 2823−2829.
(92) Walters, P. L.; Allen, T. C.; Makri, N. Direct Determination of Discrete Harmonic Bath Parameters from Molecular Dynamics Simulations. *J. Comput. Chem.* **2017**, *38* (2), 110−115.
(93) Skochdopole, N.; Mazziotti, D. A. Functional Subsystems and Quantum Redundancy in Photosynthetic Light Harvesting. *J. Phys. Chem. Lett.* **2011**, *2* (23), 2989−2993.
(94) Moix, J.; Wu, J.; Huo, P.; Coker, D.; Cao, J. Efficient Energy Transfer in Light-Harvesting Systems, III: The Influence of the Eighth Bacteriochlorophyll on the Dynamics and Efficiency in FMO. *J. Phys. Chem. Lett.* **2011**, *2* (24), 3045−3052.
(95) Shabani, A.; Mohseni, M.; Rabitz, H.; Lloyd, S. Efficient Estimation of Energy Transfer Efficiency in Light-Harvesting Complexes. *Phys. Rev. E* **2012**, *86* (1), No. 011915.
(96) Panitchayangkoon, G.; Voronine, D. V.; Abramavicius, D.; Caram, J. R.; Lewis, N. H. C.; Mukamel, S.; Engel, G. S. Direct Evidence of Quantum Transport in Photosynthetic Light-Harvesting Complexes. *Proc. Natl. Acad. Sci. U.S.A.* **2011**, *108* (52), 20908−20912.
(97) Sarovar, M.; Ishizaki, A.; Fleming, G. R.; Whaley, K. B. Quantum Entanglement in Photosynthetic Light-Harvesting Complexes. *Nat. Phys.* **2010**, *6* (6), 462−467.
(98) Maiuri, M.; Ostroumov, E. E.; Saer, R. G.; Blankenship, R. E.; Scholes, G. D. Coherent Wavepackets in the Fenna−Matthews−Olson Complex Are Robust to Excitonic-Structure Perturbations Caused by Mutagenesis. *Nat. Chem.* **2018**, *10* (2), 177−183.
(99) Frenkel, J. On the Transformation of Light into Heat in Solids. I. *Phys. Rev.* **1931**, *37* (1), 17−44.
(100) Popp, W.; Brey, D.; Binder, R.; Burghardt, I. Quantum Dynamics of Exciton Transport and Dissociation in Multichromophoric Systems. *Annu. Rev. Phys. Chem.* **2021**, *72* (1), 591−616.
(101) Hernández, F. J.; Crespo-Otero, R. Modeling Excited States of Molecular Organic Aggregates for Optoelectronics. *Annu. Rev. Phys. Chem.* **2023**, *74* (1), 547−571.

https://doi.org/10.1021/acsomega.3c09720
ACS Omega 2024, 9, 9666−9675

(102) Read, E. L.; Schlau-Cohen, G. S.; Engel, G. S.; Wen, J.; Blankenship, R. E.; Fleming, G. R. Visualization of Excitonic Structure in the Fenna-Matthews-Olson Photosynthetic Complex by Polarization-Dependent Two-Dimensional Electronic Spectroscopy. *Biophys. J.* **2008**, *95* (2), 847−856.
(103) Ishizaki, A.; Fleming, G. R. Theoretical Examination of Quantum Coherence in a Photosynthetic System at Physiological Temperature. *Proc. Natl. Acad. Sci. U.S.A.* **2009**, *106* (41), 17255−17260.

https://doi.org/10.1021/acsomega.3c09720
ACS Omega 2024, 9, 9666−9675